Exploring the effects of ZVI addition on resource recovery in the anaerobic digestion process

Puyol, D.; Flores-Alsina, Xavier; Segura, Y.; Molina, R. ; Padrino, B. ; Fierro, J. L. G. ; Gernaey, K. V.; Melero, J. A.; Martinez, F.

Published in:
Chemical Engineering Journal

Link to article, DOI:
10.1016/j.cej.2017.11.029

Publication date:
2018

Document Version
Peer reviewed version

Exploring the effects of ZVI addition on resource recovery in the anaerobic digestion process

D. Puyol, X. Flores-Alsina, Y. Segura, R. Molina, B. Padrino, J.L.G. Fierro, K.V. Gernaey, J.A. Melero, F. Martinez

PII: S1385-8947(17)31941-1
DOI: https://doi.org/10.1016/j.cej.2017.11.029
Reference: CEJ 18000

To appear in: *Chemical Engineering Journal*

Received Date: 20 September 2017
Revised Date: 3 November 2017
Accepted Date: 4 November 2017

Please cite this article as: D. Puyol, X. Flores-Alsina, Y. Segura, R. Molina, B. Padrino, J.L.G. Fierro, K.V. Gernaey, J.A. Melero, F. Martinez, Exploring the effects of ZVI addition on resource recovery in the anaerobic digestion process, *Chemical Engineering Journal* (2017), doi: https://doi.org/10.1016/j.cej.2017.11.029

Exploring the effects of ZVI addition on resource recovery in the anaerobic digestion process

D. Puyol[1,1], X. Flores-Alsina[2], Y. Segura[1], R. Molina[1], B. Padrino[1], J.L.G. Fierro[3], K.V. Gernaey[2], J.A. Melero[1], F. Martinez[1]

[1] Group of Chemical and Environmental Engineering (GIQA). Rey Juan Carlos University, Madrid, Spain

[2] Process and Systems Engineering Center (PROSYS), Technical University of Denmark, Building 229, DK-2800 Kgs. Lyngby, Denmark.

[3] Sustainable Energy and Chemistry Group (EQS), Instituto de Catálisis y Petroleoquímica, CSIC, Madrid, Spain

Abstract

The influence of Zero Valent Iron (ZVI) addition on the potential resource recovery during the anaerobic digestion (AD) of domestic waste sludge is assessed. Potentially recoverable resources analyzed were nutrients such as struvite to recover P, and energy as biogas to recover C. Short term (biochemical methane potential tests, BMP) and long term (AD1, AD2) experiments are conducted using two types of set-up (batch, continuous). Process data (influent, effluent and biogas) is continuously collected and the dry digested sludge is analyzed by XPS. A mathematical model is developed based on a modified version of the Anaerobic Digestion Model No 1 upgraded with an improved physicochemical description, ZVI corrosion, propionate uptake enhancement and multiple mineral precipitation. The results of all experiments show that ZVI addition increases methane production and promotes the formation of siderite ($FeCO_3$) and vivianite ($Fe_3(PO_4)_2$), which causes changes in the biogas composition (%CH_4

[1] Corresponding author information: daniel.puyol@urjc.es. Room 234, Dep. Build. I (Mostoles), Mostoles Campus, C/ Tulipan, S/n, 28933, Mostoles, Madrid, Spain

versus $\%CO_2$) and reduces P release. The model can satisfactorily reproduce the dynamics of AD processes, nutrient release, pH and methanogenesis in AD1. The proposed approach also describes the changes in the overall performance of the process because of ZVI addition in AD2. A model-based scenario analysis is included balancing chemical-ZVI addition and increased methane production/struvite precipitation. This scenario analysis allows concluding that: (a) the improvement of methane production does not compensate the costs of ZVI purchase, and (b) ZVI dramatically decreases the P recovery potential in the digestate of the AD systems. This is the first study to experimentally and mathematically describe the effect of ZVI on biogas production/composition and on the fate of phosphorus compounds, and its potential implications for potential energy and phosphorus recovery in AD systems.

KEYWORDS

Model-based evaluation; BMP; phosphorus recovery; Anaerobic Digestion; ADM1

NOMENCLATURE

AD = Anaerobic Digestion

AD1 = Anaerobic digestion under study without ZVI addition

AD2 = Anaerobic digestion under study with ZVI addition

ADM1 = Anaerobic digestion model No 1

BMP = Biochemical Methane Potential

BSM2 = Benchmark Simulation Model No 2

CG – TCD = Gas chromatography

CH_4 =Methane measurements (g CH_4 d^{-1})

$CHEM_i$ = Chemical cost, i = ZVI, NaOH, $MgOH_2$, $MgNH_4PO_4$

CO_2 = Carbon dioxide measurements (g CO_2 d^{-1})

COD = Chemical oxygen demand (kg m^{-3})

CODsol = Soluble COD (kg m^{-3})

CODpart = Particulate COD (kg m^{-3})

G_{CH4} = Methane model predictions (g CH_4 d^{-1})

G_{CO2} = Carbon dioxide model predictions (g CO_2 d^{-1})

GC-TCD = Gas Chromatography – Thermal Conductivity Detector

ICP-OES = Inductively coupled plasma - optical emission spectrometry

ISS = Inorganic suspended solids measurements (g m^{-3})

k_H = Hydrolysis constant in BMP assays (d^{-1})

ki = Precipitation constant, i = $FeCO_3$, $Fe_3(PO_4)_2$ (d^{-1})

K_i = Solubility constant, i = $FeCO_3$, $Fe_3(PO_4)_2$ (mass-based)

MP = Methane production (kg d^{-1})

NH_4^+ = Ammonium measurements (g m^{-3})

OCI = Operational cost index (-)

PER = Potential energy recovery (kg d^{-1})

PO_4^{3-} = Phosphate measurements (g m^{-3})

S1, S2 = Scenario

S_{aa} = Amino acids (soluble) (ADM1 state variable) (kg COD m^{-3})

S_{ac} = Acetate (soluble) (ADM1 state variable) (kg COD m^{-3})

S_{bu} = Butyrate (soluble) (ADM1 state variable) (kg COD m^{-3})

S_{fa} = fatty acids (soluble) (ADM1 state variable) (kg COD m^{-3})

S_I = Inert material (soluble) (ADM1 state variable) (kg COD m^{-3})

SI = Saturation Index. SI represents the logarithm of the ratio between the product of the respective activities of reactants that are each raised to the power of their respective stoichiometric coefficients, and the solubility product constant (K_{sp}).

S_{iC} = Inorganic carbon (soluble) (ADM1 state variable) (kmol m^{-3})

S_{iN} = Inorganic nitrogen (soluble) (ADM1 state variable) (kmol m^{-3})

S_{iP} = Inorganic phosphorus (soluble) (ADM1 state variable) (kmol m^{-3})

SP = Sludge production (kg d^{-1})

S_{pro} = Propionate (soluble) (ADM1 state variable) (kg COD m^{-3})

S_{su} = Sugars (soluble) (ADM1 state variable) (kg COD m^{-3})

S_{va} = Valerate (soluble) (soluble) (ADM1 state variable) (kg COD m^{-3})

TSS = Total suspended solids measurements (g m^{-3})

VSS = Volatile suspended solids measurements (g m^{-3})

X_B = Biomass (particulate) (ADM1 state variable) (kg COD m^{-3}) (= $X_{su} + X_{aa} + X_{fa} + X_{c4} + X_{pro} + X_{ac} + X_{H2}$)

X_C = Composite material (particulate) (ADM1 state variable) (kg COD m^{-3})

X_{ch} = Carbohydrates (particulate) (ADM1 state variable) (kg COD m^{-3})

X_I = Inert material (particulate) (ADM1 state variable) (kg COD m^{-3})

X_{inf} = Inorganic material (particulate) coming with the influent (g m^{-3})

X_{li} = Lipids (particulate) (ADM1 state variable) (kg COD m^{-3})

X_{prot} = Proteins (particulate) (ADM1 state variable) (kg COD m^{-3})

XPS = X-ray photoelectron spectroscopy

ZVI = Zero valent iron

1. INTRODUCTION

Anaerobic digestion (AD) is a mature technology for bioenergy production (through biogas) that is mostly implemented as waste sludge stabilization method in wastewater treatment plants, as well as for direct bioenergy production from energy crops. The economic feasibility of AD is generally related to the achievable methane yields, and current research in AD is devoted to intensification techniques to enhance biogas production through different approaches [1]. Beside obvious initial choice of

improvement of reactor configuration and operation conditions, great advances are made in the use of alternative feedstocks to expand AD application within the bioenergy sector.

Novel feedstocks include hardly-biodegradable microbial biomass as microalgae, phototrophic bacteria and high-loaded adsorption sludge (A-stage sludge), and solid organic waste as the organic fraction of the municipal solid waste, lignocellulosic biomass or petroleum hydrocarbons [2]. During AD, organic biodegradable material is biologically degraded in absence of oxygen following four different steps, and producing biogas. Among the different steps involved in AD (hydrolysis, acidogenesis, acetogenesis and methanogenesis), enzymatic reduction of complex organic compounds to simpler and soluble molecules during hydrolysis is usually the limiting step of the process. Therefore, multiple methods have been explored to improve the hydrolysis, both thermal as well as physical-chemical [3].

Pre-treatments of the sludge (hydrothermal treatments, oxidative processes, etc.) have been proposed as alternative to increase biodegradability and overall kinetics of the biomethanation processes occurring during AD [4]. Among these alternatives, the use of zero-valent iron (ZVI) has become a promising option due to its low cost if ZVI originates from waste, ease of application (direct contact with the waste sludge) and its capacity to decrease oxidative–reductive potential (ORP) of the anaerobic digestion media and therefore provide a more favorable environment for anaerobic digestion [5]. Moreover, iron is a cofactor of several enzymatic activities occurring in the fermentation stage during acidogenesis [6]. Actually, ZVI enhances the biochemical methane potential (BMP) of organic feedstocks due to its action as electron donor by corrosion, generating H_2 that can be used by hydrogenotrophic methanogens, sulfate reducing bacteria or dechlorinating bacteria [7]. This reduces the overall redox state of

the system, and it has been claimed to improve significantly the hydrolysis of the hardly-biodegradable fraction of the organic waste [8]. Additionally, the process acts as a buffer of the acid produced by acidogens, which is a crucial step to maintain a stable and favorable condition for methanogenesis, and consequently improving the BMP in the AD system [9]. Recently, it has been also demonstrated that ZVI stimulates the activity of acidogenic bacteria, as demonstrated with the increase of specific enzymatic activities of several key enzymes involved in fermentation and anaerobic oxidation pathways [10]. Therefore, ZVI acts as an enhancer of the overall fermentation activity, but particularly the propionate fermentation, thus regulating the concentration of propionate that also enhances the activity of other anaerobic microorganisms (especially methanogens).

However, during the ZVI corrosion process Fe^{2+} is released and strongly influences the physicochemical properties of the system [11]. Fe^{2+} can reduce the biogenic sulfide due to pyrite precipitation (FeS_2), but can also interact with other anions, notably bicarbonate and phosphate, to form siderite ($FeCO_3$) and vivianite ($Fe_3(PO_4)_2 \cdot 8H_2O$) [12]. Vivianite precipitation entraps the soluble P released upon AD. Though this reduces P contamination in the main line, most importantly it also reduces the P recovery potential due to accumulation of vivianite in the stabilized sludge, whose subsequent recovery is difficult and costly. This theoretical process has never been considered as a problem in the use of ZVI for AD enhancement, even though a similar reaction system between Fe^{3+}-Fe^{2+}-P has been widely demonstrated to occur in anoxic soils [13]. Nevertheless, the increasing general concern about P availability for human beings makes it difficult to justify significant losses of P recovery potential in return for an increase of the methane potential.

Thus, the aim of this work is to analyze the effects of ZVI addition on the energy and P recovery potentials from waste activated sludge upon AD following two experimental strategies: i) BMP and kinetics of the AD in batch experiments in the absence/presence of ZVI; and ii) two lab-scale anaerobic digestion systems under continuous operation in the absence/presence of ZVI (AD1, AD2) treating domestic waste sludge. A mathematical model describing the main biological and physicochemical processes is then developed, and the model performance is evaluated by comparing simulation results with experimental results. Finally, two scenarios of AD using ZVI are studied in order to assess how ZVI might alter potential energy and phosphorus recovery strategies.

2. MATERIALS AND METHODS

2.1. Biomass sources

Waste sludge was collected from a domestic wastewater treatment plant (DWWTP) in Madrid, Spain. The sludge was characterized as follows: 23±6 kgTSS m^{-3}, 8±1 kg VSS m^{-3}, 6±1 kg COD m^{-3}, 250±60 g NH_4^+-N m^{-3} and 14±6 gPO_4^{3-}-P m^{-3}. The inoculum was extracted from the full-scale anaerobic digestion unit of the aforementioned DWWTP.

2.2. Biochemical methane potential assays

BMP assays were carried out according to Segura et al. [4] for evaluating methane yield and phosphate dissolution in the digestate under different conditions: i) only domestic secondary sludge (sample raw); ii) the sludge in the presence of two different concentrations of ZVI (2.5 and 10 kg m^{-3}, samples Fe2.5 and Fe10, respectively); and iii) the sludge with both ZVI concentrations but also spiking additional phosphorus as phosphate (10 g P m^{-3}, samples Fe2.5P10 and Fe10P10, respectively). Batch digestions were performed in 100 mL working volume non-stirred bottles at 37±0.5 ºC. All assays were carried out in triplicate.

2.3. Anaerobic digestion in continuous mesophilic reactors

Two identical 2 L continuously fed anaerobic digesters were used under mesophilic conditions (37±0.5 ºC) to treat domestic secondary sludge. AD1 is used as control. In AD2 the effect of ZVI addition was explored. Model predictions are calibrated using two data sets comprised of 87 days. Operational conditions of studied variables in this work and the dynamic conditions of the inlet streams for the two experimental set-ups are summarized in Table 1, whereas the full characterization of the influent can be found in Supporting Information.

2.4. Analytical methods

Total and soluble COD, alkalinity and TSS/VSS were measured according to standard methods [14]. NH_4^+ and PO_4^{3-} were quantified by using Merck kits (Merck, Darmstadt, Germany). Biogas production in continuous reactors was measured by liquid-gas Milligascounters (Ritter, Bochum, Germany). Analysis of gas production in BMP tests was performed by using Boyle-Mariotte pressure meters, according to Segura et al. [4], whereas biogas composition was analyzed by GC-TCD. Soluble Fe^{2+}, Ca^{2+}, Mg^{2+}, K^+ and Na^+ were quantified by ICP-AES. Elemental composition, chemical and electronic state of the elements in the dry solid fraction of the digestate was analyzed by X-ray photoelectron spectroscopy (XPS). Details of the experimental procedure to record and process spectra are given elsewhere [15].

2.5. Anaerobic digestion model

The Benchmark Simulation Model No 2 (BSM2) implementation of Anaerobic digestion model no 1 (ADM1) [16, 17] is selected to describe the anaerobic digestion process. Phosphorus is modelled using a source-sink approach assuming a predefined elemental (C, H, N, P, O) composition [18]. Phosphorus (secondary substrate/nutrient) limitation is included in all the uptake rates. The model also includes ZVI corrosion [19]

and propionate uptake enhancement [7]. The original composite material variable (X_C) is removed and decay products are directly mapped into biodegradable (X_{prot}, X_{li}, and X_{ch}) and inert (X_I) organics [20]. Total Solids (TSS) is described as a predicted variable separating the volatile (VSS) of the inorganic solids (ISS) [21]. The ADM1 is also upgraded with an improved physicochemical description. This framework is comprised of: i) a speciation/complexation aqueous-phase chemistry model [22]; and ii) a multiple mineral precipitation model [23, 24]. The first model quantifies pH and describes ionic behavior by extensive consideration of non-ideality, including ion activities instead of molar concentrations and ion complexation/pairing. In the second model, precipitation is described as a reversible process using the saturation index (SI) as the driving force. SI represents the logarithm of the ratio between the product of the different activities (reactants) and the solubility product constant (K_{sp}).

2.6. Data management and statistical analysis

All the batch tests were done in triplicate. Experimental data are presented as arithmetic means. Error bars in experimental data represent 95% confidence intervals in mean values based on a two-tailed t-test (5% significance threshold).

Kinetic parameters of methane production in BMP assays were obtained by fitting first order models to the data as per Segura et al. [4], thereby calculating k_H (in d^{-1}) and BMP (B_0, in g CH_4 (kg TSS)$^{-1}$, which corresponds to 1.244 NL CH_4 (kg TSS)$^{-1}$). Parameter uncertainty was determined using two-tailed t-tests calculated from the standard error in the parameter value, obtained from the Fisher information matrix. Where parameter optimization problems involve multiple parameters (k_H, BMP), parameter uncertainty surface (J = Jcrit, 5% significance threshold) has also been assessed as described in [25]. Confidence intervals (at 95%) were also calculated based on two-tailed t-tests from the parameter standard error, as above, and used for statistical representative

comparisons. All the statistical analyses of BMP assays were performed by using Aquasim 2.1d.

The modified ADM-1 model was implemented in Matlab-Simulink using a three-level approach [26]. Firstly, a graphical user interface is created to link the different models as block diagrams. Second, model parameter values and post-processing data routines are developed using the Matlab language (m-files). Finally, biological and physicochemical models (ADM, PCM) are implemented in the C language to ensure a fast-computational speed. Ode15s is used to solve the system of ordinary differential equations. A multi-dimensional implementation of the Newton Raphson method solves the physicochemical speciation model.

3. RESULTS

3.1. Biochemical methane potential tests (BMP)

Figure 1 shows the results obtained in the BMP assays. The effect of ZVI was analyzed from three different perspectives: i) effect on the methane production and the kinetic parameters (k_H and BMP; Figure 1a and 1b, respectively); ii) variation of the dissolved phosphate concentration upon the end of the experiment (Figure 1c); and iii) variation of the biogas composition (Figure 1d).

ZVI increased the methane production as compared to the control experiment. This resulted into a significant increase of the BMP when adding 2.5 kg ZVI m^{-3}. However, a further increase of the ZVI concentration (from 2.5 to 10 kg ZVI m^{-3}) induced a significant reduction in the biogas production (Figure 1b) probably attributed to the predominance of toxic effects of the added ZVI on the microbial consortium. It is also noteworthy that the ZVI did not modify the kinetics of the process, as the k_H values did not vary significantly in the presence of ZVI. These observations are in agreement with previous work, which postulates that ZVI mainly enhances the methane potential

introducing electrons into the system but it does not improve the hydrolysis kinetic of the anaerobic digestion process [27]. Moreover, a recent work hypothesizes that ZVI can enhance the hydrolysis of refractory compounds [10]. Since the substrate used here (domestic waste sludge) is easily biodegradable, this effect seems to be unappreciable. The extra addition of 10 g P m^{-3} did not have a significant effect either.

The release of phosphate was affected by the ZVI, obtaining a considerable reduction in PO_4^{3-} concentration in the digestate in the presence of the iron (from ca. 22 g P m^{-3} in the case of the control experiment to 3.5 and 5.0 g P m^{-3} for 2.5 and 10 kg ZVI m^{-3}, respectively). These results seem to indicate that the released PO_4^{3-} is not significantly affected when the ZVI concentration is above 2.5 kg ZVI m^{-3}. Moreover, when additional phosphorus in a dose of 10 g P m^{-3} was added besides ZVI, the phosphorus concentration in solution decreased to values not significantly different than those mentioned previously (ca. 3 and 4.4 g P m^{-3} for Fe2.5P10 and Fe10P10 experiments, respectively). However, dissolved Fe under these conditions was significantly lowered compared to the experiments in the absence of additional phosphorus addition, suggesting the increased formation of precipitates with Fe and P when dosing extra phosphorus.

Finally, the biogas composition changed dramatically in the presence of ZVI during the anaerobic digestion (Figure 1d). The CO_2 proportion decreased with increased ZVI concentrations, being almost negligible when 10 kg ZVI m^{-3} were added. This provides an indication of the interaction between Fe and CO_2.

3.2.Experimental results in continuous reactors (AD1, AD2)

The results obtained in the continuous anaerobic digesters are shown in Figure 2, whereas a summary of key parameters is shown in Table 2. As a general observation,

there are statistical evidences indicating that the mechanisms observed in batch are valid for continuous reactors as well.

In this case, the benefit of ZVI in terms of methane production is hardly observed during the first 2 operative stages. From day 29 onwards, this trend particularly changed and during stage 2 and 3 the increase of methane production was evident when adding ZVI to the digester, resulting in average CH_4 production values around 12% higher in the AD2 reactor compared to the AD1 reactor (Table 2); this increase is significant at 95% confidence.

Production of CO_2 was also decreased in the AD2 reactor compared to the AD1 reactor, though this trend was also evident in the operative stages 1 and 2, where significant decreases of the average CO_2 production of 23 and 13%, respectively, were observed.

The decrease of the dissolved phosphorus concentration in the digestate stream was considerably higher than that obtained in batch assays. This was not evident during the first stage, probably due to the accommodation of the reactors to the dynamic conditions. However, the continuous addition of ZVI in the AD2 caused a critical decrease of the soluble P in the outlet stream, with average concentration values that are around 60% lower than in the AD1 reactor during stage 2. This was even more noticeable when extra phosphorus was added to the inlet sludge stream in the operative stages 3 and 4. During these periods, the values of phosphate detected in the digestate of the AD2 reactor not only decreased as compared to the AD1 reactor, but also achieved values lower than 14 g P m^{-3}, which was the background value of the dissolved phosphate in the sludge before anaerobic digestion. A chemical characterization of the sludge precipitates was performed to know more on the mechanism of CO_2 and soluble P variability.

Characterization of dried digestate by XPS during stage 3 revealed the presence of C, N, O, P, Ca, Si and Fe in both AD1 and AD2 (see SI). The binding energies of the elements in both AD1 and AD2 samples indicate that the main P species binds metal phosphates, O binds also to phosphorus, carbonates and organics, N binds organic N, and Fe binds FeS-type compounds. C principally binds in organic compounds (at 284.8 eV), though the proportion of inorganic C in AD2 (as carbonate/bicarbonate with binding energy of 287 eV) increased due to the presence of ZVI (from 13% in AD1 to 20 and 24% in AD2 in the presence and absence of extra P, respectively). The Fe2p core-level spectra ($2p_{3/2}$ and $2p_{1/2}$) of samples from AD1 and AD2 shows no satellite lines (Figure 3), which is commonly observed for low spin configurations of Fe(II) [28], which contrasts with high-spin Fe(III) compounds which have always satellite structures [29]. Also, binding energies for iron could be assigned to low dispersed Fe^{2+} ions. This essentially means that almost all the Fe present in the samples of both reactors is Fe(II).

4. DISCUSSION

4.1. Main outcomes and hypothesis

The main outcomes from both the BMP and the continuous experiments are: (i) methane production was significantly increased in the presence of 2.5 kg ZVI m^{-3} (p-value < 0.05), although an excess of ZVI (10 kg ZVI m^{-3}) reduced the methane potential; (ii) methane potential (and not the hydrolysis rate) was enhanced in the presence of ZVI; (iii) CO_2 production significantly decreased in the presence of ZVI; (iv) ZVI induced the immobilization of phosphate in the solid phase; (v) binding energies of C atoms indicated an increase of inorganic C due to the presence of ZVI; (vi) Fe(II) was the unique form of Fe immobilized in the anaerobic sludge upon digestion; and, (vii) the appearance of Fe(II) in AD2 was independent of the soluble P

concentration. With these outcomes, a hypothesis about the role of ZVI on the anaerobic digestion can be extracted and formulated. The hypothesis can be summarized with the following postulates: a) ZVI is corroded to Fe^{2+} in anaerobic conditions, producing H_2 (Eq. [1]); b) ZVI stimulates the activity of anaerobic bacteria; c) H_2 is then converted into methane by hydrogenotrophic methanogens (Eq. [2]), yielding increased CH_4 production due to ZVI addition; d) Fe^{2+} precipitates with PO_4^{3-} to form vivianite ($Fe_3(PO_4)_2$) (Eq. [3]); and e) Fe^{2+} also interacts with CO_2 to form insoluble siderite ($FeCO_3$) (Eq. [4]).

$$Fe_0 + 2H^+ \rightarrow Fe^{2+} + H_2 \quad [1]$$

$$4H_2 + CO_2 \rightarrow CH_4 + 2H_2O \quad [2]$$

$$Fe^{2+} + PO_4^{3-} \rightarrow Fe_3(PO_4)_2 \quad [3]$$

$$Fe^{2+} + CO_2 + H_2O \rightarrow Fe_2CO_3 + 2H^+ \quad [4]$$

With these postulates formulated, the research question that results from the hypothesis is: Is the ZVI utilization as enhancer of the anaerobic digestion of organic waste sludge economically and environmentally feasible under the current experimental conditions? Our results and subsequent analyses are indicating that it is not. The theoretical basis for such a result is developed in the following parts.

4.2. Mechanisms

The enhancement of the BMP by the addition of ZVI reported here has been previously supported and evidenced in the literature [8, 10]. The direct production of H_2 from ZVI corrosion in non-oxidative environments has been described as a mechanism for this enhancement [30]. A recent work has postulated that the direct enhancement of the enzymatic activity of anaerobic bacteria is the main cause of the BMP increase [10], especially the propionate acetogens [7]. Although this was previously explained by the improvement of the environmental redox conditions, since ZVI can considerably

decrease the ORP [6], this explanation has been recently discarded [10]. As such, the increase of the process rate has been questioned, as the ZVI seems to affect to the BMP only [27]. Additionally, there are no convincing evidences indicating that ZVI increases universally hydrolysis rates, as has been depicted in Figure 1d, and therefore ZVI addition should not be viewed as a method for improvement of the methane production rate (since the hydrolysis is the limiting step of the AD process).

Under anaerobic conditions, water can oxidize ZVI to ferrous ions and generate hydrogen gas, as shown by the negative standard Gibbs free energy change, and then Fe^{2+} can interact with water ions to form ferrous hydroxides [31]. However, Fe^{2+} will bind preferentially with some other anions such as HCO_3^-/CO_3^{2-}, SH^-/S^{2-} and $H_2PO_4^-/HPO_4^{2-}/PO_4^{3-}$, and therefore precipitation of different salts occurs, as predicted by the physical-chemical software module for wastewater [23, 24].

The mechanisms described and experimentally supported have been used for proposing a new model based on the ADM-1. The calibration and validation of the model is described below.

4.3.Modelling of continuous reactors

4.3.1. Influent fractionation and parameter adjustment

Influent characterization is based on the considerations taken in [32]. S_{su} (40%) and S_{fa} (60%) are assumed from COD_{sol}. S_I is estimated from COD_{sol} in the effluent. A similar procedure (from effluent COD_{part}) is used to estimate the non-biodegradable fraction (X_I) and to distinguish it from the biodegradable (X_{ch}, X_{prot} & X_{li}) fraction. TSS and VSS values in the influent are used to estimate the fraction of inorganics coming with the influent (X_{inf}). S_{iC}, S_{iN} and S_{iP} values are obtained from alkalinity, NH_4^+ and PO_4^{-3} measurements, respectively. ADM1 parameter values are adjusted using the first data set (AD1) (hydrolysis, acidogenesis, acetogenesis, methanogenesis and nutrient release).

This parameter set is used in AD2 to further adjust corrosion, enhanced acidogenesis & multiple mineral precipitation.

4.3.2. Dynamic simulations

Figure 2a depicts the dynamic profiles of the simulated model for AD1. Simulation results show that the proposed approach is capable of reproducing hydrolysis (see COD_{part}, TSS and VSS profiles), acidogenesis and acetogenesis (see COD_{sol}). The pH, CH_4 and CO_2 profiles reveal the correct description of the weak acid base chemistry, mass transfer (liquid-gas), and methanogenic (hydrogenotrophic / acetoclastic) processes by the model. The model also predicts N (see NH_4^+ profile) and P (see PO_4^{-3} profile) release with good agreement to experimental results.

Default values (not considering X_C as stated in Batstone et al. [20]) for hydrolysis rates (k_{carb}, k_{prot}, k_{lip}) could capture the dynamics of TSS/VSS indicating a correct estimation of particulate (organic/inorganic) state variables (X_{ch}, X_{pro}, X_{li}, X_I, X_B and X_{inf}). Uptake rates/affinity constants for acidogenic and acetogenic bacteria had to be increased/decreased (double) in order to match S_{su}, S_{aa}, S_{fa} and VFA (= S_{va} + S_{bu} + S_{pro} + S_{ac}) profiles with the measured COD_{sol} and biogas (CH_4 & CO_2) values (see SI). The N content in X_{pr}/S_{aa} and the P content in X_{li} were left to their default values [16].

The model may generally reproduce the trends of the monitored variables for AD1. Indeed, experimental/simulated COD_{sol}, COD_{part}, TSS, VSS, pH, PO_4^{-3}, CH_4 and CO_2 have an R^2 >0.7 (see SI). Only NH_4^+ has a lower value, most probably due to an incorrect assessment of the protein content in the influent, their particular hydrolysis rates or an incorrect assessment of the uptake of amino acids.

Figure 2b shows the dynamic profiles for the second continuous system (AD2). The good agreement between the measured (dotted lines) and the simulation results (solid lines) supports the claim that the developed model properly captures the increase in

methane production due to ZVI corrosion and enhanced propionate uptake. This is supported by a recent work, where the stimulation of the activity of acidogenic bacteria has been evidenced [10]. The model is also capable to reflect the major changes due to precipitation. The variation in the biogas composition (% CH_4 versus % CO_2) and P release (lower values) are a result of the formation of siderite ($FeCO_3$) and vivianite ($Fe_3(PO_4)_2$). Indeed, the model identified high saturation indexes (SI) values for both compounds. SI represent the logarithm of the ratio between the product of the respective activities of reactants that are each raised to the power of their respective stoichiometric coefficients. In the model, precipitation is described as a reversible process using SI as the chemical driving force. Model results also correspond with the results of the XPS analysis. Finally, the role of precipitation is also reflected in the TSS, VSS and ISS (TSS-VSS) dynamics. Again, for almost all the monitored variables, comparison of model prediction with experimental data shows a good correlation ($R^2 > 0.7$).

The parameter set employed for AD1 is also used to simulate influent and operational conditions of AD2. ZVI corrosion is formulated to be a fast process and occurs chemically. Propionate uptake enhancement increases acetogenesis rates, thus stimulating the acidogenic bacteria activity [10]. ZVI related parameters are taken from Liu et al. [7]. Precipitation constants (K_{FeCO3} and $K_{Fe3(PO3)2}$) are adjusted to match CO_2 and PO_4^{-3} measurements.

From a modelling point of view, this study demonstrates that the proposed approach is capable to reproduce the experimental data from both anaerobic systems (AD1, AD2). Special additions in the original model structure of the well-recognized ADM1 are necessary in order to describe the changes in the process performance caused by ZVI, namely enhanced methane production and reduction in the P release as well as changes in the biogas composition due to precipitation. Hence, a proper physicochemical

description of the system is absolutely necessary to correctly reproduce the experimental results. Indeed, this is the main difference with respect to previously published models [7, 19] where those effects could not be included.

4.4.Scenario analysis

The additional simulations presented in this scenario analysis (S1, S2) demonstrate the potential of using the proposed approach when performing model-based studies. Therefore, for exemplary purposes, the adjusted model will be used to: i) quantify different (process-related) evaluation criteria; and ii) explore the implications of changing the original flow diagram. More specifically, Scenario 1 (S1) presents the impact of ZVI on potential energy recovery with special emphasis on process economics. In Scenario 2 (S2), the effects of ZVI are evaluated assuming the addition of a subsequent struvite crystallization unit in order to recover phosphorus.

4.4.1. S1: Effect of different ZVI additions on energy recovery

In this section, model predictions (AD1, AD2) are used to quantify sludge production (SP), methane production (MP), potential energy recovery (PER), chemical costs (CHEM) and the operational cost index (OCI) [33]. Results summarized in Table 3 show that the addition of ZVI improves MP and PER as a result of increased acetogenic/hydrogenotrophic activity. However, SP and CHEM are increased as a trade-off. SP is higher due to a major ISS fraction in the TSS due to metal precipitation ($FeCO_3$, $Fe_3(PO_4)_2$). CHEM is higher due to the periodic purchase of ZVI. The combined OCI indicates that for this particular case the cost for external addition of ZVI does not seem to be compensated by the potential increase of the energy recovery that can be obtained from increased methane production.

4.4.2. S2: Effect of different ZVI additions on P recovery

The second scenario (S2) implies a modification of the system configuration assuming the addition of a P recovery unit. Hence, an ideal dewatering unit (DEW) after the AD1 / AD2 is included [34] to simulate potential precipitation from AD centrate. An ideal crystallizer (CRYST) is necessary to reproduce the struvite formation [35]. The assumed hydraulic retention time of CRYST units is approximately 18 h [36]. Operational pH is modified by controlling external NaOH addition. Struvite precipitation is promoted by the external addition of magnesium salts. Kinetic precipitation parameters are retrieved from previous studies [23]. The response surfaces depicted in Figure 4 show the obtained simulation results. Indeed, Figure 4a reveals that the potential quantity of P recovered as struvite in AD1 depends on magnesium concentration and operational pH. At high Mg concentration, most struvite precipitates. Higher pH values also increase the release of free ions from their paired forms and facilitate the formation of precipitates. When the Mg loads become higher than 0.05 kg d^{-1} the situation changes and the main limiting factor is P availability (it is basically all consumed). Hence, no substantial increase in the formation of precipitates is possible and adding more Mg is just an extra cost with no benefit at all. A similar observation is reported by Van Rensburg et al. [37]. In the second system (AD2), there is no formation of struvite for all the evaluated Mg dosage rates / pH values. This is mainly due to the fact that P preferentially binds with the available Fe^{2+} resulting from ZVI corrosion, to form vivianite. Addition of Fe^{2+} to anaerobic digesters to precipitate P, and hence control struvite precipitation, has been successfully demonstrated at full-scale by Mamais et al. [38]**.** The same study also proved that the salts do not re-solubilize making P not available for downstream processes (for example in the centrifuges) [37]. Only in the presence of sulfides, it seems that P can be released again due to the strong

affinity of Fe to form iron sulfides FeS, which was not the case in the experiments performed in this study [39].

4.4.3. Limitations of the study

The reader should be aware that the results of the scenario analysis should be interpreted with care and are specific for the current experimental conditions. First, there was only a little amount of sulfur in the influent wastewater. It is well-known that under anaerobic conditions, sulfate (SO_4^{2-}) is reduced to sulfides ($H_2S/HS^-/S^{2-}$) by means of sulfate reducing bacteria (SRB). The latter compete with methanogens for the same source of electron donors (H_2, VFAs). In addition, hydrogen sulfide (H_2S) at high concentration is inhibitory/toxic and may cause corrosion and odor problems. The strong affinity of Fe^{2+} with S^{2-} to form iron sulfides (FeS) converts ZVI in a very promising control method [40]. Second, the original formulation of the evaluation criteria used in section 4.4 has been done for a full-scale system, not a lab-scale system. Therefore, there might be some scaling problems, and this is particularly important when assessing the PER and the quantity of recovered struvite. However, it gives a good indication of the potential effects and therefore we decided to use those performance evaluation tools as a process performance indicator. Finally, it should be mentioned that ZVI addition was not optimized in any way. Perhaps smarter ZVI dosing strategies could offset the unfavorable increase of chemical costs and sludge production with the enhancement of methane production.

5. CONCLUSIONS

ZVI addition to anaerobic digestion systems caused Fe^{2+} to be released. This increases the BMP. Fe^{2+} interacts with PO_4^{3-} and CO_2 to form vivianite and siderite. A model is developed, including the whole AD process, ZVI corrosion, enhanced propionate uptake, liquid-gas mass transfer, weak acid-base chemistry and multiple mineral

precipitation. The impact of ZVI on potential energy and phosphorus recovery was analyzed through simulation of several cases, demonstrating that the increase of methane production did not compensate the costs of ZVI purchase, and indicating that ZVI dramatically reduces P precipitation as struvite since P is already sequestered as vivianite.

6. SUPPLEMENTARY INFORMATION (SI)

E-supplementary data of this work can be found in the online version of the paper.

7. SOFTWARE AVAILABILITY

The MATLAB/SIMULINK code of the models presented in this paper is available upon request, including the implementation of the physical-chemical and biological modelling framework in ADM1. To express interest, please contact Dr. X. Flores-Alsina (xfa@kt.dtu.dk) or Professor Krist V. Gernaey (kvg@kt.dtu.dk) at the Technical University of Denmark (Denmark).

8. ACKNOWLEDGEMENTS

The authors greatly acknowledge the Spanish Ministry of Economy and the Madrid's Community for the funding obtained through the projects CTQ2014-54563-C3-1-R (WATER4FOOD) and S2013/MAE-2716 (REMTAVARES), respectively. Dr. D. Puyol also acknowledges the Spanish Ministry of Economy for the postdoctoral grant received. Dr. X. Flores-Alsina gratefully acknowledges the financial support of the collaborative international consortium WATERJPI2015 WATINTECH of the Water Challenges for a Changing World Joint Programming Initiative (Water JPI) 2015 call. The REWARD project funded by Innovation Fund Danmark is also acknowledged.

9. REFERENCES

[1] J.M. Lema, S. Suarez, Innovative Wastewater Treatment & Resource Recovery Technologies: Impacts on Energy, Economy and Environment, IWA Publihing, 2017.

[2] J.B. Holm-Nielsen, T. Al Seadi, P. Oleskowicz-Popiel, The future of anaerobic digestion and biogas utilization, Biores. Technol. 100 (2009) 5478-5484.

[3] A. Cesaro, V. Belgiorno, Pretreatment methods to improve anaerobic biodegradability of organic municipal solid waste fractions, Chem. Eng. J. 240 (2014) 24-37.

[4] Y. Segura, D. Puyol, L. Ballesteros, F. Martínez, J. Melero, Wastewater sludges pretreated by different oxidation systems at mild conditions to promote the biogas formation in anaerobic processes, Environ. Sci. Pollut. Res. 23 (2016) 24393-24401.

[5] G. Zhen, X. Lu, Y.-Y. Li, Y. Liu, Y. Zhao, Influence of zero valent scrap iron (ZVSI) supply on methane production from waste activated sludge, Chem. Eng. J. 263 (2015) 461-470.

[6] Y. Liu, Y. Zhang, X. Quan, Y. Li, Z. Zhao, X. Meng, S. Chen, Optimization of anaerobic acidogenesis by adding Fe 0 powder to enhance anaerobic wastewater treatment, Chem. Eng. J. 192 (2012) 179-185.

[7] Y. Liu, Y. Zhang, B.-J. Ni, Zero valent iron simultaneously enhances methane production and sulfate reduction in anaerobic granular sludge reactors, Water Res. 75 (2015) 292-300.

[8] Y. Feng, Y. Zhang, X. Quan, S. Chen, Enhanced anaerobic digestion of waste activated sludge digestion by the addition of zero valent iron, Water Res. 52 (2014) 242-250.

[9] G. Zhen, X. Lu, Y.-Y. Li, Y. Liu, Y. Zhao, Influence of zero valent scrap iron (ZVSI) supply on methane production from waste activated sludge, Chem. Eng. J. 263 (2015) 461-470.

[10] X. Hao, J. Wei, M.C.M. van Loosdrecht, D. Cao, Analysing the mechanisms of sludge digestion enhanced by iron, Water Res. 117 (2017) 58-67.

[11] H. Jia, G. Yang, H.-H. Ngo, W. Guo, H. Zhang, F. Gao, J. Wang, Enhancing simultaneous response and amplification of biosensor in microbial fuel cell-based upflow anaerobic sludge bed reactor supplemented with zero-valent iron, Chem. Eng. J. 327 (2017) 1117-1127.

[12] J.S. An, Y.J. Back, K.C. Kim, R. Cha, T.Y. Jeong, H.K. Chung, Optimization for the removal of orthophosphate from aqueous solution by chemical precipitation using ferrous chloride, Environ. Technol. 35 (2014) 1668-1675.

[13] L. Heiberg, C.B. Koch, C. Kjaergaard, H.S. Jensen, B.H. Hans Christian, Vivianite precipitation and phosphate sorption following iron reduction in anoxic soils, J. Environ. Qual. 41 (2012) 938-949.

[14] APHA, Standard methods for the examination of water and wastewater, American Public Health Association (APHA), Washington, DC, USA 2005.

[15] Y. Segura, F. Martínez, J. Melero, J.G. Fierro, Zero valent iron (ZVI) mediated Fenton degradation of industrial wastewater: treatment performance and characterization of final composites, Chem. Eng. J. 269 (2015) 298-305.

[16] D.J. Batstone, J. Keller, I. Angelidaki, S.V. Kalyuzhnyi, S.G. Pavlostathis, A. Rozzi, W.T.M. Sanders, H. Siegrist, V.A. Vavilin, The IWA Anaerobic digestion Model No 1 (ADM1), in, IWA Publishing, 2002.

[17] C. Rosen, D. Vrecko, K.V. Gernaey, M.N. Pons, U. Jeppsson, Implementing ADM1 for plant-wide benchmark simulations in Matlab/Simulink, Water Sci. Technol. 54 (2006) 11-19.

[18] M. de Gracia, L. Sancho, J.L. Garcia-Heras, P. Vanrolleghem, E. Ayesa, Mass and charge conservation check in dynamic models: application to the new ADM1 model, Water Sci. Technol. 53 (2006) 225-240.

[19] X. Xiao, G.-P. Sheng, Y. Mu, H.-Q. Yu, A modeling approach to describe ZVI-based anaerobic system, Water Res. 47 (2013) 6007-6013.

[20] D.J. Batstone, D. Puyol, X. Flores-Alsina, J. Rodríguez, Mathematical modelling of anaerobic digestion processes: applications and future needs, Rev. Environ. Sci. Bio/Technol. 14 (2015) 595-613.

[21] G.A. Ekama, M.C. Wentzel, A predictive model for the reactor inorganic suspended solids concentration in activated sludge systems, Water Res. 38 (2004) 4093-4106.

[22] X. Flores-Alsina, C. Kazadi Mbamba, K. Solon, D. Vrecko, S. Tait, D.J. Batstone, U. Jeppsson, K.V. Gernaey, A plant-wide aqueous phase chemistry module describing pH variations and ion speciation/pairing in wastewater treatment process models, Water Res. 85 (2015) 255-265.

[23] C. Kazadi Mbamba, D.J. Batstone, X. Flores-Alsina, S. Tait, A generalised chemical precipitation modelling approach in wastewater treatment applied to calcite, Water Res. 68 (2015) 342-353.

[24] C. Kazadi Mbamba, S. Tait, X. Flores-Alsina, D.J. Batstone, A systematic study of multiple minerals precipitation modelling in wastewater treatment, Water Res. 85 (2015) 359-370.

[25] D.J. Batstone, P.F. Pind, I. Angelidaki, Kinetics of thermophilic, anaerobic oxidation of straight and branched chain butyrate and valerate, Biotechnol. Bioeng. 84 (2003) 195-204.

[26] J.B. Copp, The COST Simulation Benchmark: Description and Simulator Manual: a Product of COST Action 624 and COST Action 682, EUR-OP, 2002.

[27] Y. Liu, Q. Wang, Y. Zhang, B.J. Ni, Zero valent iron significantly enhances methane production from waste activated sludge by improving biochemical methane potential rather than hydrolysis rate, Scient. Rep. 5 (2015) 8263.

[28] I. Uhlig, R. Szargan, H. Nesbitt, K. Laajalehto, Surface states and reactivity of pyrite and marcasite, App. Surf. Sci. 179 (2001) 222-229.

[29] M.C. Biesinger, B.P. Payne, A.P. Grosvenor, L.W. Lau, A.R. Gerson, R.S.C. Smart, Resolving surface chemical states in XPS analysis of first row transition metals, oxides and hydroxides: Cr, Mn, Fe, Co and Ni, App. Surf. Sci. 257 (2011) 2717-2730.

[30] X. Guan, Y. Sun, H. Qin, J. Li, I.M. Lo, D. He, H. Dong, The limitations of applying zero-valent iron technology in contaminants sequestration and the corresponding countermeasures: the development in zero-valent iron technology in the last two decades (1994–2014), Water Res. 75 (2015) 224-248.

[31] Y. Yang, C. Zhang, Z. Hu, Impact of metallic and metal oxide nanoparticles on wastewater treatment and anaerobic digestion, Environ. Sci. Proc. Imp. 15 (2013) 39-48.

[32] I. Nopens, D.J. Batstone, J.B. Copp, U. Jeppsson, E. Volcke, J. Alex, P.A. Vanrolleghem, An ASM/ADM model interface for dynamic plant-wide simulation, Water Res. 43 (2009) 1913-1923.

[33] K.V. Gernaey, U. Jeppsson, P.A. Vanrolleghem, J.B. Copp, Benchmarking of control strategies for wastewater treatment plants, IWA Publishing, 2014.

[34] U. Jeppsson, M.N. Pons, I. Nopens, J. Alex, J.B. Copp, K.V. Gernaey, C. Rosen, J.P. Steyer, P.A. Vanrolleghem, Benchmark simulation model no 2: general protocol and exploratory case studies, Water Sci. Technol. 56 (2007) 67-78.

[35] C. Kazadi Mbamba, X. Flores-Alsina, D. J. Batstone, S. Tait, Validation of a plant-wide phosphorus modelling approach with minerals precipitation in a full-scale WWTP, Water Res. 100 (2016) 169-183.

[36] G. Tchobanoglous, Metcalf, Eddy, F.L. Burton, H.D. Stensel, Wastewater engineering: treatment and reuse, McGraw Hill, 2003.

[37] P. Van Rensburg, E. Musvoto, M. Wentzel, G. Ekama, Modelling multiple mineral precipitation in anaerobic digester liquor, Water Res. 37 (2003) 3087-3097.

[38] D. Mamais, P.A. Pitt, Y.W. Cheng, J. Loiacono, D. Jenkins, Determination of ferric chloride dose to control struvite precipitation in anaerobic sludge digesters, Water Environ. Res. 66 (1994) 912-918.

[39] H. Ge, L. Zhang, D.J. Batstone, J. Keller, Z. Yuan, Impact of Iron Salt Dosage to Sewers on Downstream Anaerobic Sludge Digesters: Sulfide Control and Methane Production, J. Environ. Eng. 139 (2013) 594-601.

[40] J. Zhang, Y. Zhang, X. Quan, Y. Liu, X. An, S. Chen, H. Zhao, Bioaugmentation and functional partitioning in a zero valent iron-anaerobic reactor for sulfate-containing wastewater treatment, Chem. Eng. J. 174 (2011) 159-165.

Figure captions

Figure 1. Results of biochemical methane potential assays. Experimental (symbols) and first order-modeled (lines) methane production (a); 95% confidence regions for k_H and BMP values (b); and dissolved Fe and PO_4^{3-} compared to methane production (c) and biogas composition: CH_4 (squares) and CO_2 (circles) (d) at the end of the experiments. Error bars are 95% confidence intervals. ZVI concentrations are in kg Fe m^{-3}. P 10 indicates that 10 g PO_4^{3-}-P m^{-3} were added at the beginning of the experiment.

Figure 2. Experimental results (open symbols) and simulation data (continuous lines) for AD1 (a) and AD2 (b). Note that graph titles correspond to Y axes labels for improving data visualization.

Figure 3: Fe2p core-level spectra of AD1 (squares) and AD2 (circles) outlet samples in stage 3.

Figure 4. Model based evaluation of the potential P recovery in the form of struvite as a fraction of the total load entering the system for AD1 (a) and AD2 (b). The legend indicates normalized phosphorus recovery.

Figure 1 revised

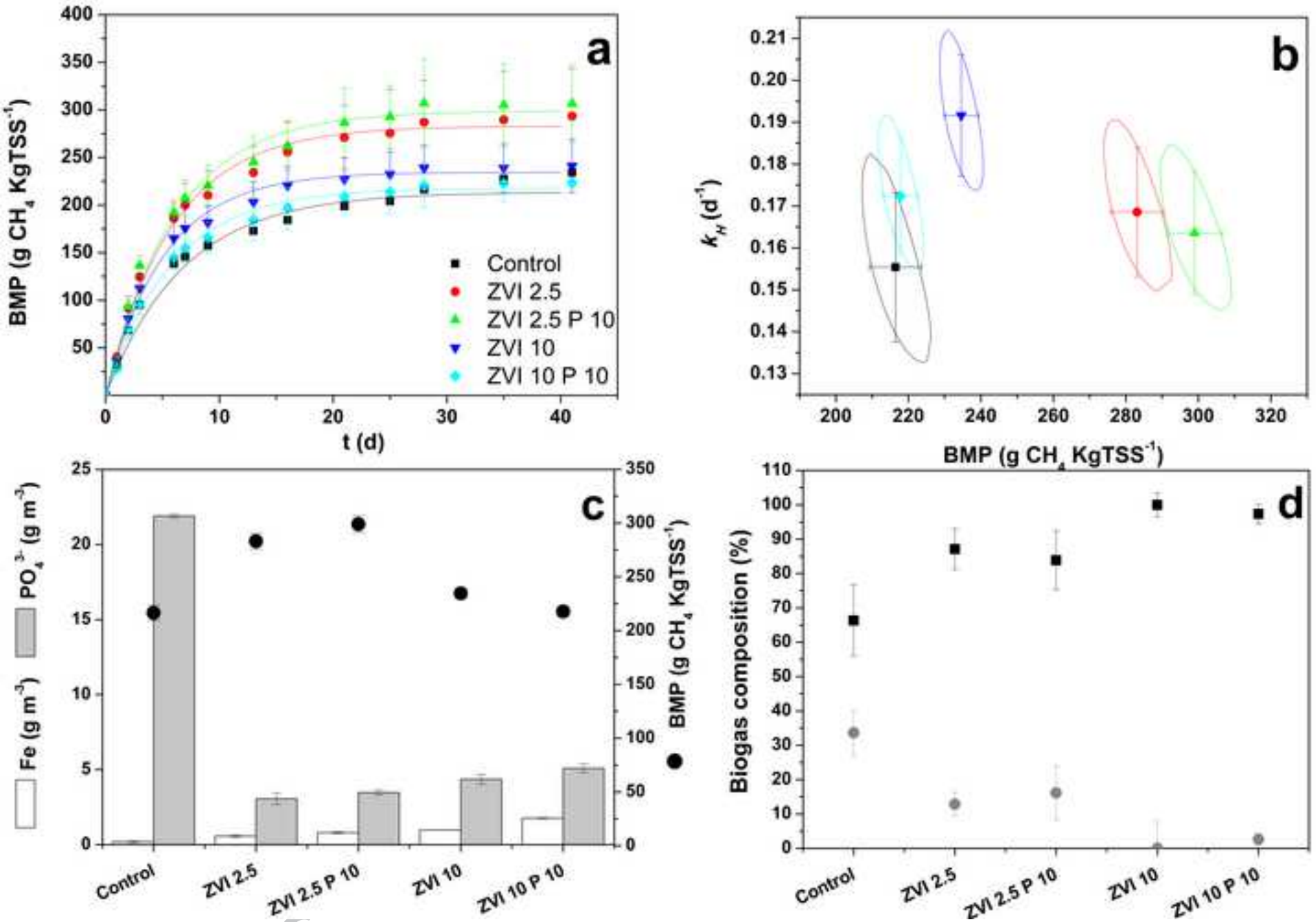

Figure 2 revised

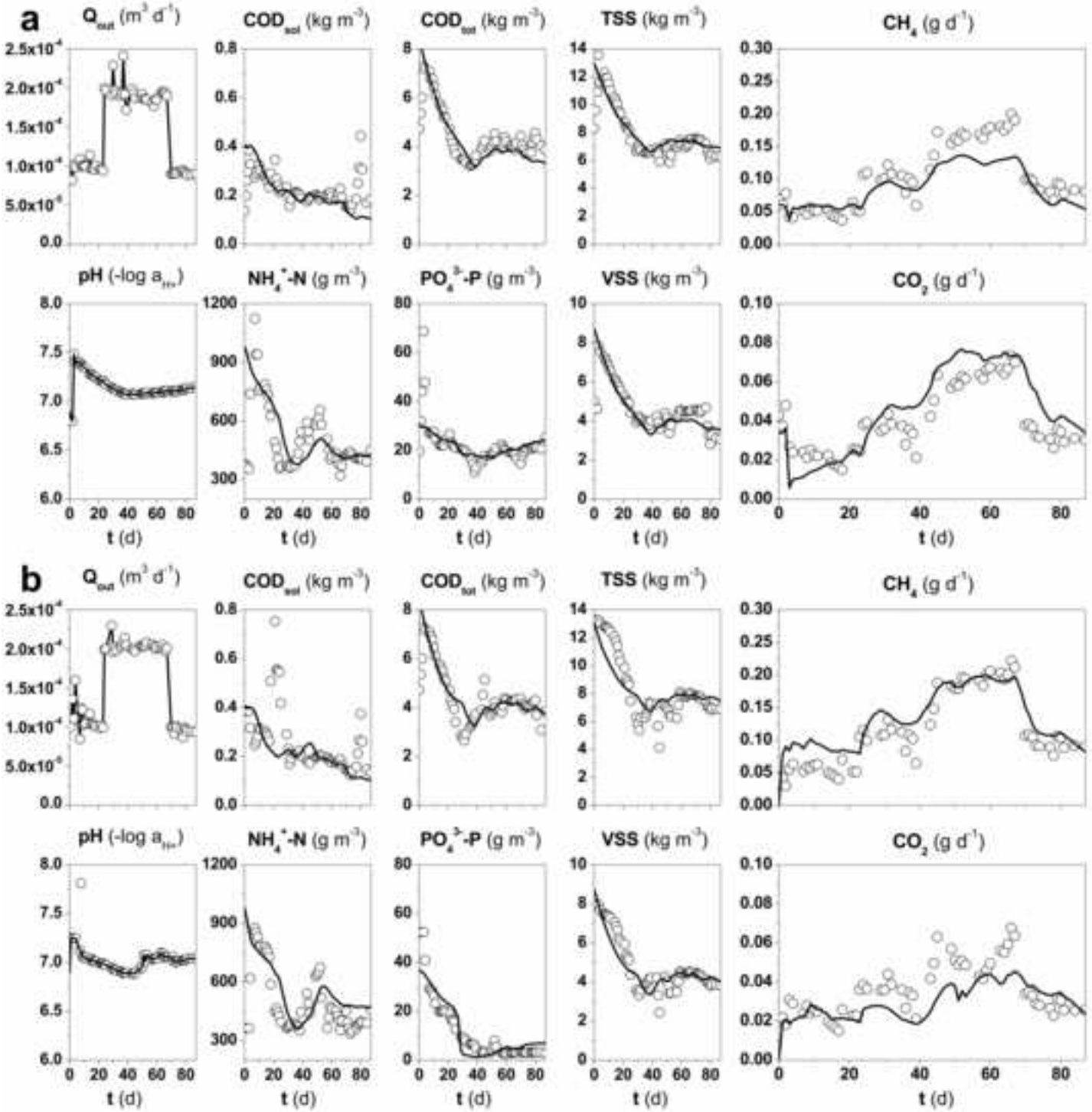

Figure 3 revised

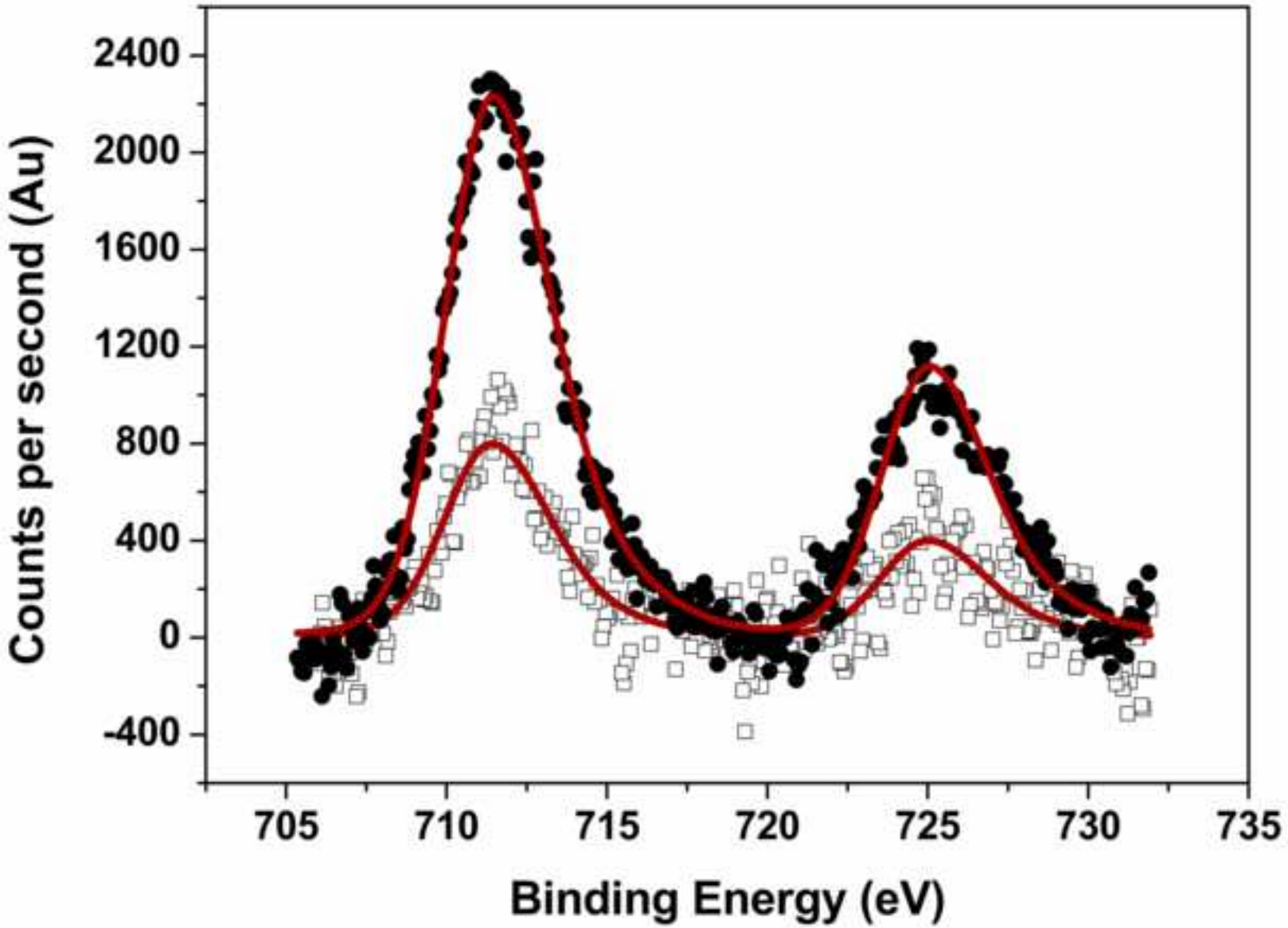

Figure 4

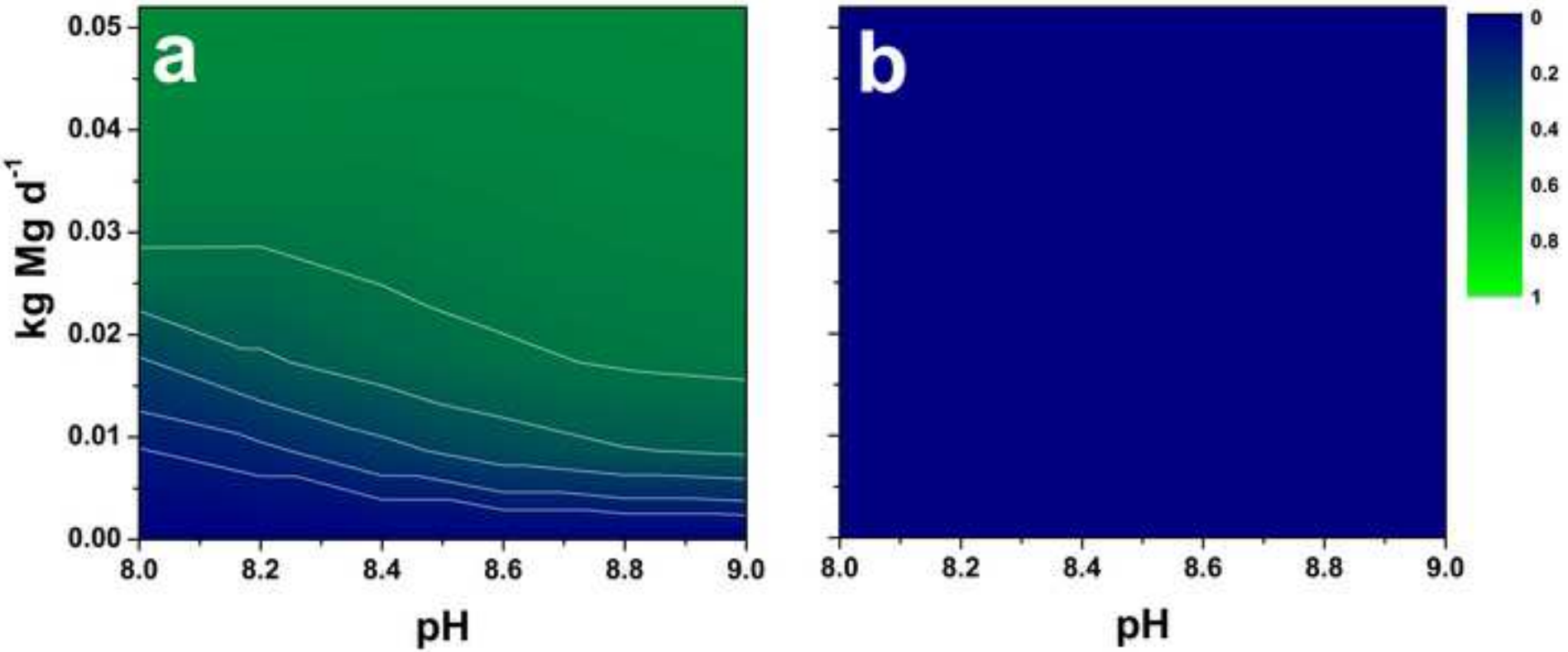

TABLES

Table 1. Experimental design of the operational conditions for the different operational stages in AD1 & AD2

STAGE	Time (d)	HRT (d)	AD1		AD2	
			ZVI (kg m^{-3})	Extra P (g m^{-3})	ZVI (kg m^{-3})	Extra P (g m^{-3})
1	20	20	-	-	2.5	-
2	24	10	-	-	2.5	-
3	21	10	-	10	2.5	10
4	21	20	-	10	2.5	10

Table 2. Summary of the main process variables for the different operational stages in the AD1 and AD2 reactors

	Stage 1	Stage 2	Stage 3	Stage 4
AD1				
CH_4 (g d^{-1})	0.051 ± 0.006	0.101 ± 0.02	0.172 ± 0.007	0.094 ± 0.02
CO_2 (g d^{-1})	0.026 ± 0.004	0.037 ± 0.006	0.064 ± 0.003	0.036 ± 0.006
pH	7.2 ± 0.2	7.12 ± 0.05	7.08 ± 0.009	7.11 ± 0.009
NH_4^+-N (kg N (kg COD in)$^{-1}$)	0.14 ± 0.05	0.09 ± 0.02	0.08 ± 0.01	0.08 ± 0.01
PO_4^{3-}-P (kg P (kg COD)$^{-1}$)	0.006 ± 0.001	0.004 ± 0.001	0.003 ± 0.001	0.004 ± 0.001
AD2				
CH_4 (g d^{-1})	0.052 ± 0.006	0.110 ± 0.02	0.195 ± 0.007	0.105 ± 0.02
CO_2 (g d^{-1})	0.023 ± 0.002	0.035 ± 0.005	0.052 ± 0.004	0.032 ± 0.006
pH	7.15 ± 0.2	6.9 ± 0.03	7.03 ± 0.009	7.03 ± 0.01
NH_4^+-N (kg N (kg CODin)$^{-1}$)	0.12 ± 0.04	0.09 ± 0.01	0.08 ± 0.01	0.08 ± 0.01
PO_4^{3-}-P (kg P (kg COD)$^{-1}$)	0.006 ± 0.002	0.0017 ± 0.001	0.0006 ± 0.0001	0.003 ± 0.001

Table 3. Evaluation criteria for the two evaluated AD systems (AD1, AD2). Conditions for the analysis are the same as the ones used in the experimental stage.

	AD1	AD2	Units
Sludge production (SP)	0.104	0.120	kg d^{-1}
Methane production (MP)	0.091	0.136	g d^{-1}
Potential Energy recovery (PER)[1]	0.0013	0.0018	kW h d^{-1}
Chemical cost (CHEM)[2]	0	0.4	g d^{-1}
Operational cost index (OCI)*10^3	308	362	-

[1] The electricity generated by the turbine is calculated by using a factor for the energy content of the methane gas (50.014 MJ (kg CH_4)$^{-1}$) and assuming a 43% efficiency for electricity generation.
[2] Relative costs for chemicals are calculated assuming a cost of 500 $/ton as ZVI (ICIS, 2016); Adaptation to OCI is arranged as described in Solon et al., 2017.

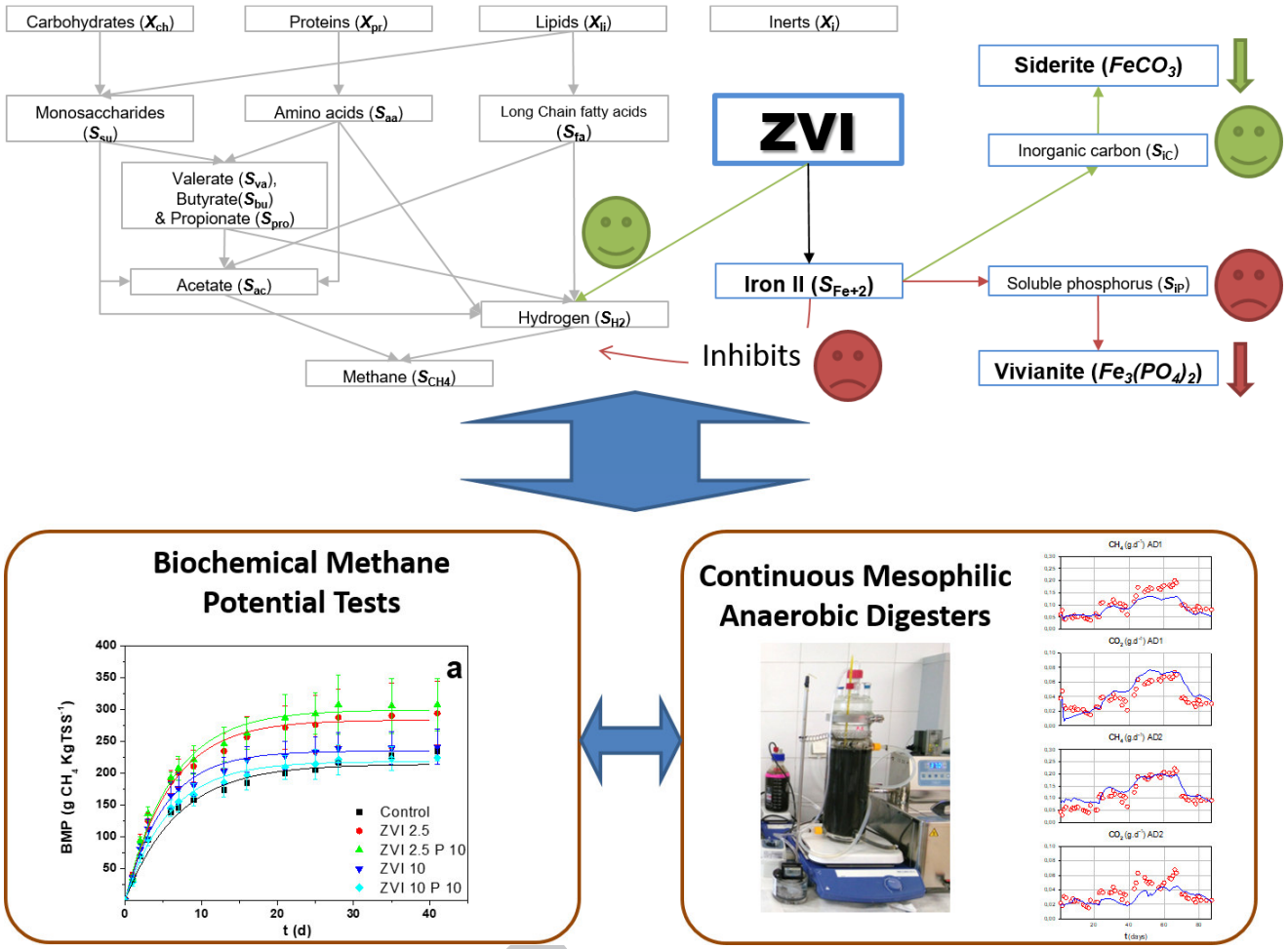

HIGHLIGHTS

- The effects of adding ZVI on batch and continuous experimental systems are analyzed
- ZVI corrosion increases CH_4 production and promotes the formation of Fe precipitates
- A model is developed and tested describing main biological and physicochemical processes
- Evaluation results show the impact of ZVI addition on potential energy and P recovery